# Spectroscopic study of $\Lambda$ hypernuclei in the medium-heavy mass region and $p$-shell region using the (e,e$'$K$^+$) reaction

**( Additional beamtime request of the approved E05-115 experiment)**


**O. Hashimoto (Spokesperson)*, S.N. Nakamura (Spokesperson), Y. Fujii, H. Kanda, M. Kaneta, D. Kawama, K. Maeda, A. Matsumura, T. Maruta, Y. Okayasu, A. Shichijo, H. Tamura, N. Taniya , K. Tsukada, T. Yamamoto, K. Yokota**

*Department of Physics, Tohoku University, Sendai, 980-8578, Japan*

**S. Kato**

*Department of Physics, Yamagata University, Yamagata, 990-8560, Japan*

**Y. Sato, T. Takahashi**

*Institute for Particle and Nuclear Physics, KEK, Tsukuba, 305-0801, Japan*

**H. Noumi**

*RCNP, Mihogaoka, Ibaraki, Osaka University, 567-0047, Japan*

**T. Motoba**

*Osaka Electro-Communication University, Neyagawa, 572-8530, Japan*

**E. Hiyama**

*Nara women's University, Nara, 630-8506, Japan*

**L. Tang (Spokesperson), I. Albayrak, O. Ates, C. Chen, M. Christy, C. Keppel, M. Kohl, Y. Li, A. Liyanage, T. Walton, Z. Ye, L. Yuan, L. Zhu**

*Department of Physics, Hampton University, Hampton, VA 23668, USA*

**J. Reinhold (Spokesperson), P. Baturin, B. Beckford, W. Boeglin, S. Dhamija, P. Markowitz, B. Raue**

*Department of Physics, Florida International University, Miami, FL 27411 USA*

**Ed.V. Hungerford**

*Department of Physics, University of Houston, Houston, TX 77204 USA*

**P. Bosted, A. Bruell, R. Ent, H. Fenker, D. Gaskell, T. Horn, M. Jones, G. Smith, W. Vulcan, S.A. Wood, C. Yan**

*Thomas Jefferson National Accelerator Facility, Newport News, VA 23606 USA*

**N. Simicevic, S. Wells**

*Department of Physics, Louisiana Tech University, Ruston, LA 71272 USA*

**B. Hu, J. Shen, W. Wang, X. Zhang, Y. Zhang**

*Nuclear Physics Institute, Lanzhou University, Gansu, China*

**J. Feng, Y. Fu, J. Zhou, S. Zhou**

*Nuclear Physics Division, China Institute of Atomic Energy, China*

**Y. Jiang, H. Lu, X. Yan, Y. Ye**

*Department of Modern Physics, University of Science & Technology of China, China*

**L. Gan**

*Department of Physics, University of North Carolina at Wilmington, Wilmington, NC 28403 USA*

**A. Ahmidouch, S. Danagoulian, A. Gasparian**

*Department of Physics, North Carolina A& T State University, Greensboro,NC 27411 USA*

**M. Elaasar**

*Department of Physics, Southern University at New Orleans, New Orleans, LA 70126, USA*

**A. Asaturyan, A. Margaryan, A. Mkrtchyan, H. Mkrtchyan, V. Tadevosyan**

*Yerevan Physics Institute, Armenia*

**D. Androic, M. Furic, T. Petkovic, T. Seva**

*University of Zagreb, Croatia*

## December 10, 2007

*** Contact person**

*Osamu Hashimoto*

*Department of Physics, Tohoku University, Sendai, 980-8578, Japan*
*hashimot@lambda.phys.tohoku.ac.jp*
*Telephone +81-22-795-6452, Fax +81-22-795-6455*

# *Proposal to JLAB PAC-33*

# Abstract

We propose an extension of the beamtime for the approved experiment E05-115 which is in preparation for beam and will be ready by the end of 2008. This experiment has been proposed and approved by PAC28 while we were taking data for it's precursor, E01-011. Meanwhile, the data analysis for E01-011 has matured and further strengthened our confidence in the proposed experimental procedure. Furthermore, we believe that recent progress in theoretical studies support our request to strengthen the impact of E05-115 by increasing the number of targets to be investigated. If approved this will increase the return on the necessary investment in time and manpower to install E05-115.

The second generation (e,e′$K^+$) hypernuclear experiment E01-011 proved the effectiveness of the (e, e′$K^+$) reaction by employing the "tilt method" for the electron arm, and by installing a new high-resolution kaon spectrometer (HKS) for the kaon arm. The E01-011 experiment performed a spectroscopic study of $\Lambda$ hypernuclei for $^{28}_{\Lambda}$Al with the (e, e′$K^+$) reaction, as the first step beyond the $p$-shell region.

As a natural extension of the successful second generation experiment, the third generation experiment E05-115 with newly developed high-resolution electron spectrometer (HES) was proposed to PAC28 in order to study $\Lambda$ hypernuclei in a wide mass region and 20 days of beamtime including commission time for a new spectrometer was accepted.

This proposal requests additional beamtime to the approved E05-115 based on recent progresses in the theoretical and experimental investigations of hypernuclei as follows:

1. Recent progresses in precise few body calculations demonstrated the importance of studying $^{7}_{\Lambda}$He and $^{10}_{\Lambda}$Be.

2. A new calculation for a $^{40}$Ca target became available and a precise mass spectrum of $^{40}_{\Lambda}$K would be needed to obtain complete $A$ dependence of $\Lambda$ single energies in the $7 \leq A \leq 52$ region.

3. Progress of the analysis/calibration methods of (e,e′$K^+$) reaction with E01-011 data suggested us to plan for more calibration data than we expected at the time of PAC28.

Therefore, we request an additional beamtime to the approved E05-115 experiment in order to carry out precision spectroscopy of $^{7}_{\Lambda}$He, $^{10}_{\Lambda}$Be, and

${}^{40}_{\Lambda}$K with sufficient calibration data. This extension beamtime will give us information about the $\Lambda N$-$\Sigma N$ coupling, charge symmetry breaking of baryon force, $\Lambda$'s glue like mechanism for neutron halo, and single particle nature of a $\Lambda$ hyperon deep inside of nucleus. The investigation will contribute greatly not only to the strangeness physics but also to the physics of unstable nuclei and astrophysics.

# 1 Physics Motivation and Experimental Objectives

## 1.1 Experimental objectives and recent theoretical progresses of hypernuclear physics

The finished second generation (e,e′K) hypernuclear experiment E01-011 took data for two targets, $^{12}$C and $^{28}$Si. The experiment proved 1) the effectiveness of the new electron spectrometer configuration, the so called "tilt method", for suppression of electron background and 2) excellent performance of the newly introduced kaon spectrometer, HKS. The success of the above improvements of (e,e′K$^+$) hypernuclear spectroscopy encouraged us to submit the third generation experiment E05-115 to PAC28.

In that proposal, we explained how hypernuclear investigation provides invaluable information on many-body hadronic systems with a new degree of freedom "strangeness" [1, 2, 3, 4]. Let us summarize briefly the unique characteristics of hypernuclear spectroscopy:

- A $\Lambda$ hyperon can be put deep inside a nucleus as an impurity and provides a sensitive probe of the nuclear interior, since it is free from Pauli blocking of the other nucleons.
- New nuclear structure, which cannot be seen in ordinary nuclei consisting only of nucleons, can manifest itself in hypernuclei, providing indispensable information on the flavor SU(3) basis for baryonic matter.
- Hyperon-nucleon ($YN$) and hyperon-hyperon ($YY$) interactions can be well studied by the spectroscopic investigation of hypernuclei.

The collaboration intended to spend most of the requested time (30 days including commissioning) on an $A \sim 50$ hypernucleus ($^{51}$V target), and the remaining beamtime for exploratory heavy target ($^{89}$Y) and a few $p$-shell targets from $^{6,7}$Li, $^{10,11}$B. The experiment was approved by PAC28 for 20 days, thus, most likely not allowing enough time to acquire sufficient data on the light targets. Based on the recent progresses of the theoretical studies, and the success of the E01-011 analysis, we would like to extend the E05-115 beamtime to acquire more data for $^{7}$Li, $^{10}$B, and $^{40}$Ca targets, together with enough calibration data. The following will outline the theoretical justification for this request.

**Study on $p$-shell hypernuclei**

It should be noted that the recent progress of theoretical studies on few-body hypernuclei allows us to calculate the binding energies of ground and excited states for lighter systems directly from free two-body interactions. Those calculations can be compared with the high accuracy experimental data.

Progresses of experimental and theoretical studies shed light on the discrepancy between experimental data and theoretical predictions of hypernuclear masses. There existed a long-standing problem that there is no $\Lambda$-N interaction model which can describe simultaneously the simple $s$-shell hypernuclei, ${}^{4}_{\Lambda}$H, ${}^{4}_{\Lambda}$He, ${}^{5}_{\Lambda}$He ground states. Akaishi *et al.* pointed out that the problem is not in ${}^{4}_{\Lambda}$H and ${}^{5}_{\Lambda}$He, but in the calculation of the ${}^{4}_{\Lambda}$He system [5]. Inclusion of the coherent $\Lambda N$-$\Sigma N$ coupling (*YNN* three-body interaction) is recognized to be essential for the calculation of the ${}^{4}_{\Lambda}$He mass. In a neutron star, the coherent $\Lambda N$-$\Sigma N$ coupling from all neutrons are quite strong and it is important to understand the effect for neutron rich hypernuclei not only for understanding of hypernuclear structure but also for neutron star structure. The study of neutron rich ${}^{7}_{\Lambda}$He hypernucleus provides such information. In the cluster picture, ${}^{7}_{\Lambda}$He can be described as $\alpha + n + n + \Lambda$ and precise four body calculation techniques developed by Hiyama *et al.* can be applied to the system [6, 7]. The first excited state $2^+$ of neutron rich ${}^{6}$He is unstable, but the above calculation predicts that by adding a $\Lambda$ as (${}^{6}$He $2^+$) + $\Lambda$ = ${}^{7}_{\Lambda}$He, the $5/2^+$ and $3/2^+$ states will be bound (Fig. 1). This is a good example of $\Lambda$'s glue role and the unbound excited neutron halo structure can be studied in this hypernucleus. The ${}^{7}$Li (e,e′K$^+$) ${}^{7}_{\Lambda}$He reaction will enable us to study such states. Furthermore, the (e,e′K$^+$) reaction with wide momentum acceptance of the HKS+HES system provides an energy calibration method by p(e,e′K$^+$)$\Lambda$ or $\Sigma^0$ reaction. The absolute $\Lambda$ binding energy information, which cannot be obtained by meson induced hypernuclear study, is quite important to extract physics information from the spectra by comparing with theoretical calculations. Wide acceptance of HKS+HES system may allow us also to search for the ${}^{7}_{\Sigma}$He hypernucleus which may be a bound state with a mass of $\sim$80 MeV heavier than ${}^{7}_{\Lambda}$He [7, 8]. Using an enriched ${}^{6}$Li target, it is possible to compare systematically hypernuclear isotopes, ${}^{7}_{\Lambda}$He and ${}^{6}_{\Lambda}$He.

Another interesting object is ${}^{10}_{\Lambda}$Be = $\alpha + \alpha + n + \Lambda$. Recent precise measurements of level differences of $p$-shell hypernuclear states by $\gamma$-ray

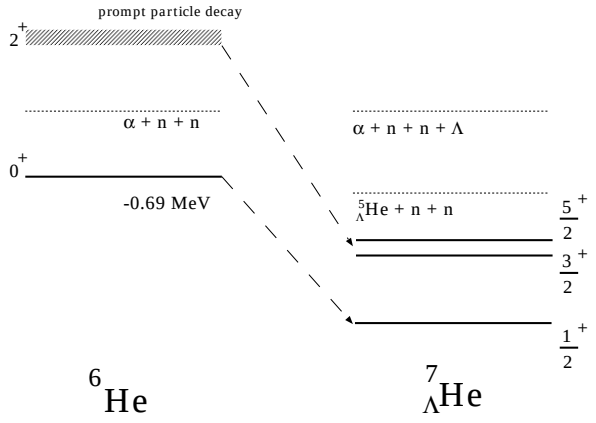


Figure 1: Energy levels for $^{6}$He and $^{7}_{\Lambda}$He [7]

spectroscopy [9] and theoretical calculations determined all parameters of the effective $\Lambda$-N potential for $p$-shell hypernuclei [10]. The obtained potential explains the existing hypernuclear structure for $A = 4, 7, 9, 13$ systems, however it failed to explain the very small level splitting ($< 100$keV) between $1^-$ and $2^-$ states of $^{10}_{\Lambda}$B. It might be caused by imperfect treatment of the tensor force originated from the non-coherent $\Lambda N$-$\Sigma N$ coupling which can be renormalized in the $\Lambda-$N interaction. We can study the tensor force by using the charge symmetry hypernucleus $^{10}_{\Lambda}$Be through the $^{10}$B(e,e′K$^+$)$^{10}_{\Lambda}$Be reaction. It should be noted that the study of $^{10}_{\Lambda}$Be excited states is interesting from a view point of $\Lambda$'s glue role to the $^{9}$Be unbound neutron halo states like $^{7}_{\Lambda}$He case.

It is particularly important to study these hypernuclei with thin enriched targets and obtain information on the isospin dependence of the structure. The high quality electron beam allows us to use much thinner enriched target which cannot be used with meson beams.

In such studies, information on light $\Lambda$ hypernuclear structure obtained by spectroscopic studies plays an essential role in testing and improving $YN$ interaction models. Quantitative understanding of $YN$ and $YY$ interactions is a key issue for investigation of the new aspects and new forms of hadronic matter. In particular, detailed information on $YN$ and $YY$ interactions is indispensable for our understanding of high-density nuclear matter inside neutron stars, where hyperons are possibly mixed and playing crucial roles.

**Beyond $p$-shell hypernuclei**

In the investigation of hadronic many-body systems with strangeness, there is a fundamental question, "to what extent does a $\Lambda$ hyperon keep its identity as a baryon inside a nucleus?" [11]. Spectroscopic data in heavier hypernuclei can help to answer this question. Indeed, the relevance of the mean-field approximation in nuclear physics is one of the prime questions related to role that the sub-structure of nucleons plays in the nucleus. The mean-field dynamics dominates the structure of medium ($A \geq 16$) and heavier ($A \geq 40$) nuclei and $\Lambda$ hypernuclei prove the existence of single-particle motion from the deepest $s$-orbit up to large $L$ valence orbits. The existing data from $(\pi^+, \mathrm{K}^+)$ reactions obtained at KEK, however, do not resolve the fine structure in the missing mass spectra due to limited energy resolution (a few MeV), and theoretical analyses suffer from those uncertainties. The improved energy resolution ($< 400$keV) of (e,e′K$^+$) hypernuclear spectroscopy, which is comparable to the spreading widths of the excited hypernuclear states, will provide the following:

- mass dependence of the central binding potential depth from the well calibrated absolute $\Lambda$ binding energies,
- information about the spin-orbit splitting as a function of the core nucleus mass,
- distinguish between effects from the static spin-orbit potential and dynamical self-energies due to core polarization,
- self-consistent interaction parameters for non-relativistic Hartree-Fock or relativistic mean-field theories.

Effective masses of a $\Lambda$ hyperon in the nuclear potential will be obtained, which appears to be closer to that of the free value in contrast to the case of ordinary nuclei. Therefore, the proposed precision measurement of the single particle levels can address the degree of non-locality of the effective $\Lambda$-Nucleus potential and also can be compared, for example, with the advanced mean field calculations based on the quark-meson coupling (QMC) model by Thomas *et al.* [12] and on DDRH by Lenske *et al.* [13]. This can be related to the nature of the $\Lambda$N and $\Lambda$NN interactions, and to the $\Lambda$N short range interactions [14]. In a more exotic way, the binding energies were discussed in terms of the distinguishability of a $\Lambda$ hyperon in nuclear

medium, which will result in a different $A$ dependence of the binding energy as suggested by Dover [15].

Figure 2 shows that $A$ dependence of $\Lambda$ single particle energies calculated by mean-field theories with various parameters [12, 13]. In the $A \rightarrow \infty$ limit, *i.e.* infinite matter, the ambiguity due to parameters in the relativistic mean field theories becomes smaller and reliable experimental input from the light to medium-heavy region is quite important. One can see that the E01-011, the approved E05-115, and here the proposed experiments will provide high precision experimental data which cover wide $A$ region almost uniformly, ${}^{6,7}_{\Lambda}$He, ${}^{10,11}_{\Lambda}$Be, ${}^{12}_{\Lambda}$B, ${}^{16}_{\Lambda}$N, ${}^{28}_{\Lambda}$Al, ${}^{40}_{\Lambda}$K, and ${}^{52}_{\Lambda}$V. The resolutions of the existing data by the ($\pi^+$,K$^+$) reaction are a few MeV and the (e,e′K$^+$) data with 3-400 keV resolution and reliable absolute binding energy will provide the precious parameters for those calculations.

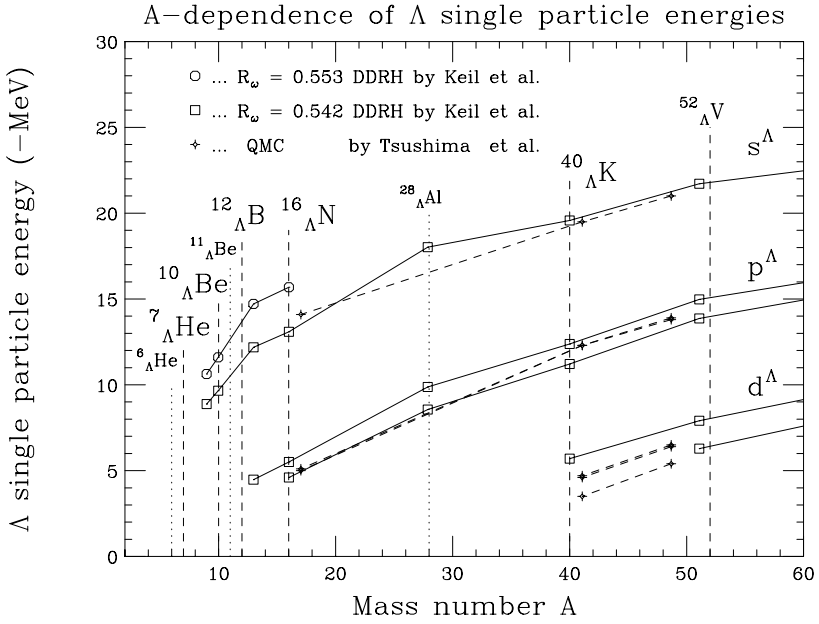


Figure 2: The calculated $A$ dependence of $\Lambda$ single particle energies of $s^{\Lambda}, p^{\Lambda}, d^{\Lambda}$ states for various hypernuclei [12, 13]

We will also study the unique structure of medium-heavy $\Lambda$ hypernuclei and possible spin-orbit splitting of the $\Lambda$ single particle states in these hypernuclei. The ${}^{89}$Y spectra taken by the $(\pi^+, \mathrm{K}^+)$ reaction show that the higher $l$ states are split by about 1 MeV. These splittings are suggested to be due to the $\Lambda$N $ls$ interaction, although the magnitude of the splitting is much larger than expected from previous measurements in the $p$-shell hypernuclei. The splitting was also interpreted as due to an interplay of different neutron hole states as suggested by a recent theoretical calculation [16]. With a

resolution of 3-400 keV, we will try to entangle closely degenerate hypernuclear states, and clarify the origin of the splittings. If the origin of the splitting is due to $ls$ interaction it will give us the magnitude of the interaction. If the splitting is due to core excitation, it will give us information on the characteristic hypernuclear structure of medium-heavy hypernuclei. In either case, new features of $\Lambda$ hypernuclei will be investigated.

The (e,e′K$^+$) hypernuclear study provides complementary and unique information to the existing meson induced hypernuclear experiments and future J-PARC experiments, since it converts proton to $\Lambda$. Elementary process of the strangeness electro-production occurs at a bound proton and various hypernuclear states will be populated in the (e,e′K$^+$) reaction. Selecting an adequate target as a simple proton-neutron core, we can expect simple, but information rich excitation spectra for the electro-produced hypernuclei. The (e,e′K$^+$) spectroscopy has a chance to access the genuine hyperon interactions.

Recent theoretical calculations for photo-production of $^{28}$Si($\gamma$,K$^+$)$^{28}_{\Lambda}$Al, $^{40}$Ca($\gamma$,K$^+$)$^{40}_{\Lambda}$K and $^{52}$Cr($\gamma$,K$^+$)$^{52}_{\Lambda}$V were performed by Bydzovsky *et al.* [17]. Our momentum transfer is quite small ($Q^2 \sim 3 \times 10^{-6}$ GeV$^2/c^2$) and kinematics of the proposed experiment is quite similar to that of the photo-production process. The spectra of those targets are expected to be simple and easy for analysis. Especially $^{40}_{\Lambda}$K is clean, since the $^{40}$Ca target is doubly $LS$-closed up to the $0d_{3/2}$ shell.

Figure 3 shows the calculated $^{40}$Ca($\gamma$,K$^+$)$^{40}_{\Lambda}$K excitation function and it shows major peaks of $2^+, 3^-, 4^+$ which correspond to $s^{\Lambda}_{1/2}, p^{\Lambda}_{3/2}$ and $d^{\Lambda}_{5/2}$ states. We can extract precise $\Lambda$ single-particle energies from those peaks in medium heavy region. Careful comparison between data and theoretical calculations about sub-peaks of $2^-$ and $3^+$ will give information about spin-orbit splitting or core-configuration mixing.

The $^{52}$Cr target has four protons in $0f_{7/2}$ shell and neutron $jj-$closed, and major peaks will be originated from conversion of a $0f_{7/2}$ proton to $\Lambda$ in $s, p, d$ and $f$ orbits. Therefore, a clean spectrum can be expected for $^{52}$Cr(e,e′K$^+$)$^{52}_{\Lambda}$V reaction, too. Therefore, we are currently considering to take data on $^{52}$Cr for an $A \sim 50$ target instead of $^{51}$V as originally requested in E05-115 proposal. It should be noted that this part of the program is already covered by the approved E05-115.

Hypernuclear spectroscopy is a quite powerful tool for the quantitative investigation of these basic questions of hadronic many-body systems.

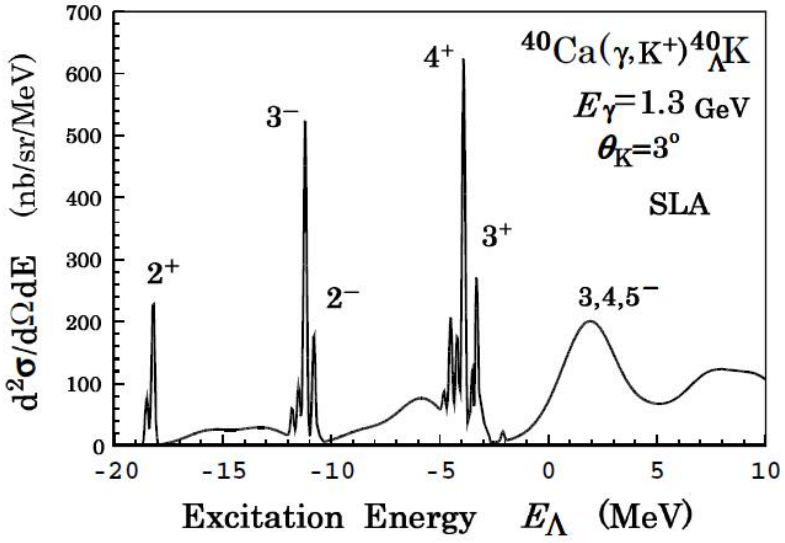


Figure 3: Calculated $^{40}$Ca($\gamma$,K$^+$)$^{40}_{\Lambda}$K excitation function by DWIA with SLA model. The calculation assumed $E_\gamma = 1.3$ GeV, $\theta_K^L = 3^\circ$ and $ls$-splitting of $0.17(2\ell + 1)$ MeV [17].

## 2 The (e, e′K$^+$) reaction for the hypernuclear spectroscopy

Since the momentum transfer of the (e,e′K$^+$) reaction is almost the same as that of the $(\pi^+, \mathrm{K}^+)$ reaction, it is expected to preferentially populate high-spin bound hypernuclear states similarly to the $(\pi^+, \mathrm{K}^+)$ reaction. However, in contrast to the reactions with meson beams, the (e, e′K$^+$) reaction will populate spin-flip hypernuclear states as well as non-spin-flip states, since the transition operator has spin-independent ($f$) and spin-dependent ($g$) terms [19, 20].

Another characteristics of the (e,e′K$^+$) reaction is that it converts a proton to a $\Lambda$ hyperon, in contrast to the ($\pi^+$,K$^+$) and $(\mathrm{K}^-, \pi^-)$ reactionreactions. This results in proton-hole-$\Lambda$-particle states in the configuration $[(lj)_N^{-1}(lk)^\Lambda]_J$. When the proton hole state is $j_> = l + 1/2$, the highest spin states of $J = J_{max} = j_> + j_>^\Lambda = l_N + l_\Lambda + 1$ are favorably excited. These hypernuclear states are of unnatural parity when the original proton orbit is $j_>$. On the other hand, if the hole state has spin $j = j_< = l - 1/2$, the highest spin states of the multiplet $J'_{max} = j_< + j_>^\Lambda = l_N + l_\Lambda$ with natural parity are strongly populated. This selectivity is particularly important as it allows us to directly study the spin-dependent structure of $\Lambda$ hypernuclei.

Experimentally, the most important characteristics of the (e,e′K$^+$) reaction is that it can potentially achieve significantly better energy

resolution because the reaction is initiated with a primary electron beam of extremely good beam emittance; it is in contrast to secondary meson beams. Combined with high performance spectrometers, an energy resolution of a few 100 keV can be achieved. Another experimental advantage is that electro-production of $\Lambda$ and $\Sigma^0$ from a proton can be used as absolute missing mass calibration due to the large momentum acceptance of the HKS and HES spectrometers (Fig. 4). Though this absolute binding energy calibration is very important, it cannot be applied for the $(K^-, \pi^-)$, ($\pi^+$,$K^+$) reactions, or for the (e, e′$K^+$) reaction with spectrometers with small acceptance.

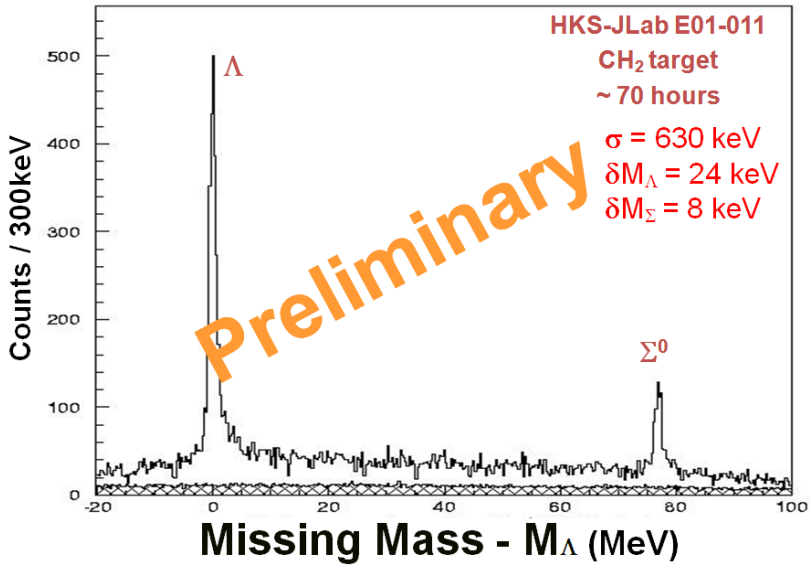


Figure 4: p(e,e′$K^+$)$\Lambda, \Sigma^0$ missing mass spectra obtained in E01-011. Wide momentum acceptance of the spectrometers allows us to have simultaneously $\Lambda, \Sigma^0$ in p(e,e′$K^+$) missing mass spectrum. Known $\Lambda$ and $\Sigma^0$ masses can be used for the absolute energy calibration. Note that the resolution for the hypernuclei is significantly better due to larger recoil mass.

The unique characteristics of the (e,e′$K^+$) reaction are summarized below.

- Extremely good energy resolution (300∼400 keV) when coupled with the kaon spectrometer (HKS) and the newly developed electron spectrometer (HES).
- Production of natural and non-natural parity states.
- Production of neutron rich hypernuclei as the reaction replaces a proton by a $\Lambda$.

- Reliable energy scale calibration by the elementary p(e,e′K$^+$)$\Lambda, \Sigma^0$ reaction in $H_2O$ or $CH_2$ targets for HKS+HES.

It is important to prepare isotopically enriched targets, *e.g.* $^6$Li and $^{10}$B for spectroscopy of neutron rich light hypernuclei. Of particular advantage for here proposed additional program on light nuclei is that the excellent beam property of CEBAF allows us to use small and thin ($<$100mg/cm$^2$) enriched targets which cannot be used by the competing meson reactions; therefore future $\gamma$ spectroscopy measurements, at for example J-PARC, are unlikely.

Although the (e,e′K$^+$) reaction has many advantages for hypernuclear spectroscopy, it had not been realized because the cross section is much smaller than reactions using hadronic beams and two high resolution spectrometers are required. For example, the calculated cross section for the $^{12}$C(e,e′K$^+$)$^{12}_{\Lambda}$B$_{gs}$ is two order of magnitude smaller than that of the corresponding $^{12}$C($\pi^+$,K$^+$)$^{12}_{\Lambda}$C$_{gs}$ reaction. Actually the hypernuclear yields of the ground state of $^{12}_{\Lambda}$B in the first generation experiment E89-009, are smaller by almost two order of magnitude compared with that of $^{12}_{\Lambda}$C by the KEK-SKS experiment. However, this disadvantage can be overcome and similar hypernuclear yield is expected with high-quality beam at CEBAF by employing a new geometry which we used successfully for the second generation E01-011 experiment and plan to adopt in the third generation experiment. The proposed experimental setup employs the High resolution Kaon Spectrometer (HKS) and also the ”tilt method” for a new electron spectrometer (HES) as described in the next section.

### 2.1 Previous (e,e′K$^+$) experiments

The first generation hypernuclear electro-production experiment E89-009 has been successfully completed at JLab Hall C in the spring of 2000. This experiment used the $^{12}$C(e,e′K$^+$)$^{12}_{\Lambda}$B reaction, and observed the ground state peak of $^{12}_{\Lambda}$B hypernucleus. The experiment demonstrated that $\Lambda$ hypernuclear spectroscopy can be performed by the (e,e′K$^+$) reaction and that sub-MeV energy resolution can be obtained for the first time in hypernuclear reaction spectroscopy.

The E89-009 experiment was designed to take advantage of the peak in the virtual photon flux at very forward angles. Therefore, it had low luminosity since a maximum number of photons/incident electron were available for reactions. Zero degree electrons and positive kaons were bent

into their respective spectrometers on opposite sides of the beam by a splitter magnet. The electron momentum was analyzed by a small Split-Pole spectrometer (Enge) positioned to detect zero degree electrons. Positive kaons were detected also at around 0 degrees using the SOS spectrometer. The experiment utilized a low beam current of 0.66 $\mu$A with a $^{12}$C target 20 mg/cm$^2$ thick.

Although the experiment was successful, the yields were limited due to the background flux of bremsstrahlung in the electron spectrometer. We had recognized that further improvement of the experimental configuration would be required to extend these studies to heavier systems. The first generation experiment E89-009 provided valuable information on rates and cross sections in order to design a geometry for the second generation experiment.

In 2005, the second generation experiment, E01-011 at Hall C took data with a newly designed kaon spectrometer, HKS and a new electron spectrometer configuration, tilt method. The tilt method successfully reduced bremsstrahlung background from 200 MHz to 1 MHz though target thickness was increased by a factor of 5 and beam intensity by a factor of 50.

Figure 5 shows $^{12}_{\Lambda}$B spectra of the first generation E89-009 (top) and the second generation E01-011 experiment (bottom). One can see that introduction of HKS and tilt method improved drastically the resolution, statistics, and signal to noise ratio. The binding energy scale of the E01-011 spectrum has not yet been finalized, but preliminary results show $< 500$ keV (FWHM) resolution.

The analysis took longer than originally anticipated. There are two main reasons for this:

- A mistake was made when last minute changes to the spectrometer settings were made to accommodate a slightly misconfigured beam exit chicane; this resulted in a loss of statistics.
- Due to the short lifetime of $CH_2$ targets exposed to beam, more sophisticated studies like spectrometer momentum scans were not performed.

Section 5 will outline our plans to improve these calibrations.

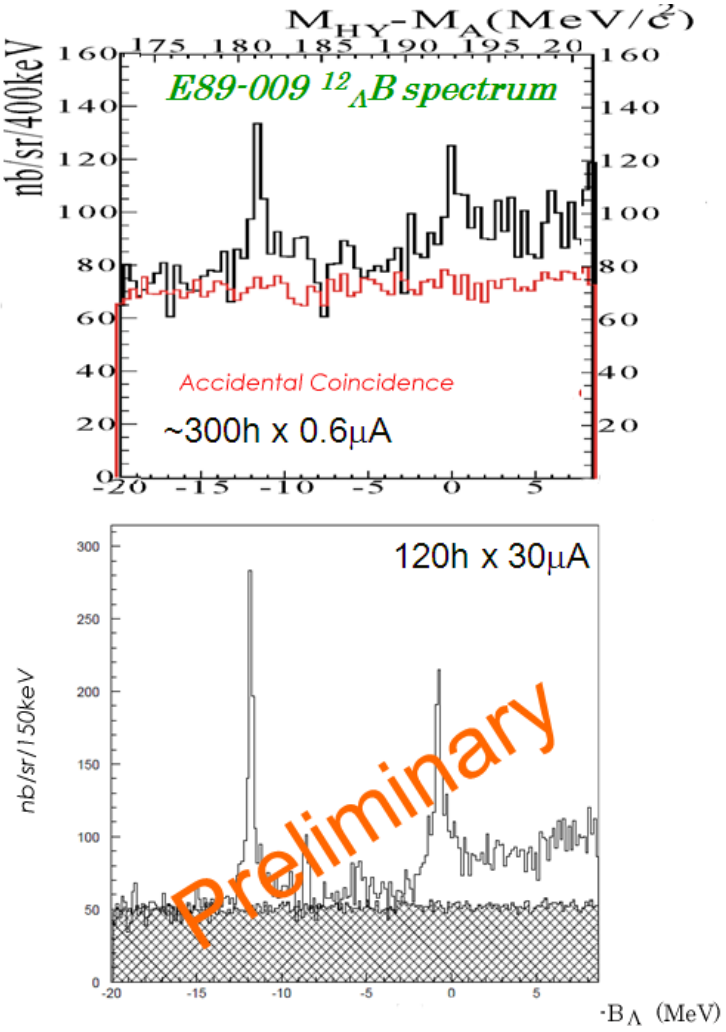


Figure 5: ${}^{12}_{\Lambda}$B spectra obtained in E89-009 (top) and E01-011 (bottom).

# 3 Proposed experiment

## 3.1 Principle of the proposed experimental

The principle of the proposed experiment is essentially the same as the second generation experiment E01-011 and what we proposed to PAC28. The improvements from the E89-009 experiment are:

- The high resolution kaon spectrometer (HKS) was installed in Hall C; it will have 10 msr solid angle combined with a newly developed splitter and simultaneously achieve $< 400$ keV (FWHM) hypernuclear mass resolution.

- Optimization of scattered electron detection angle allows us to avoid the 0-degree bremsstrahlung electrons but still measure the scattered electrons at a sufficiently forward angle. The “tilt method” in which the electron spectrometer is tilted by a few degrees vertically allows us to accept a beam current as high as a few tens $\mu$A. The tilt angle is optimized for a given experimental kinematics so that bremsstrahlung electrons and M$\phi$ller electrons do not enter the acceptance of the electron arm.

When PAC28 approved E05-115, a new high-resolution electron spectrometer (HES) was still in its design stage. Meanwhile, the construction of HES was finished (Fig. 6). The HES can accept electrons with momentum of up to 1.0 GeV/$c$ which is higher than the Enge spectrometer does. We will use HKS and the newly developed HES, taking full advantage of the “tilt method” which drastically reduced the background in E01-011.

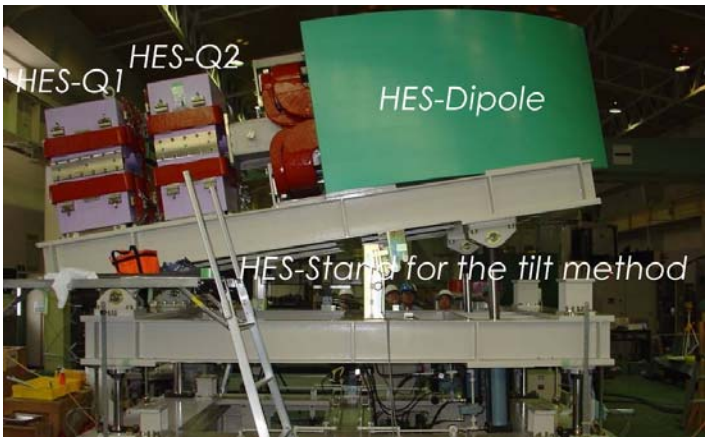


Figure 6: Completed HES magnets in Sendai, Japan. HES EQ1-EQ2-ED magnets are placed on the tilting support frame.

A plan view of the proposed geometry consisting of the new Splitter (SPL), new high resolution electron spectrometer (HES), and high resolution kaon spectrometer (HKS) is shown in Figure 7. Through intensive discussion with the accelerator group, we decided to adopt a pre-chicane beamline rather than a post-chicane, which we used for E01-011. In order to compensate deflection of the primary beam in the SPL magnet, we will adjust the beam direction before the target. Beam quality before the target is much better than it is after the target and smaller beam pipes and magnets with narrower gap can be used. Furthermore, beam diagnose tools and beam

control are much easier than with the post-chicane option.

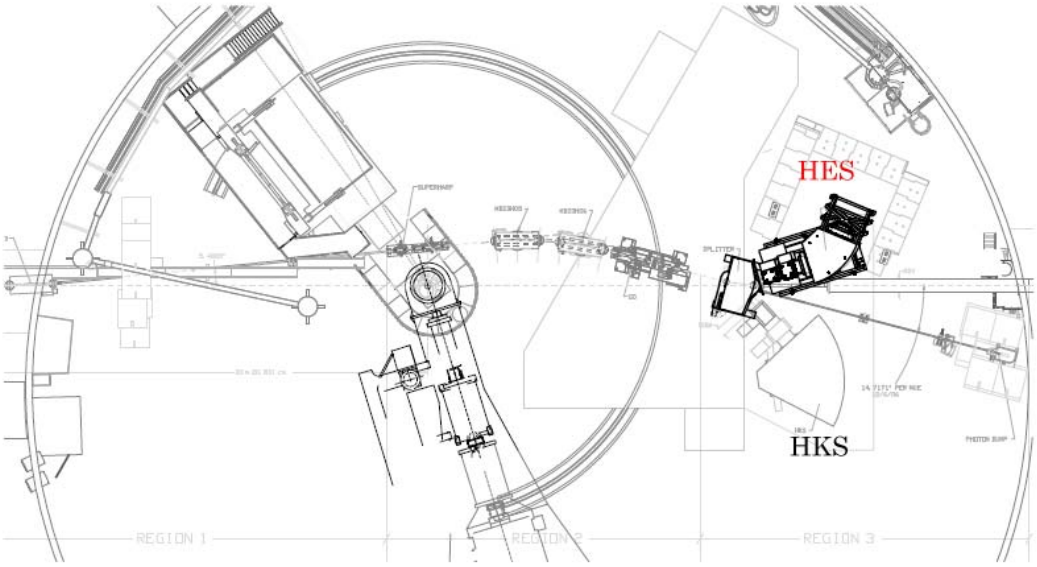


Figure 7: Floor plan of the HKS + HES + new SPL configuration in Hall C for the proposed experiment.

Both the HKS spectrometer and the HES spectrometer are positioned as forward in angle as possible without accepting 0-degree electrons or positrons. The HKS spectrometer, having a QQD configuration, was already used in E01-011 and its performed as expected. It has a momentum resolution of $2 \times 10^{-4}$ (FWHM) at 1.2 GeV/$c$, and a large solid angle of $\sim$10 msr, including the new splitter. This is summarized in Table 1.

In design of the proposed experiment, E89-009 and E01-011 data were fully utilized and singles rates of electrons, positrons, pions and protons in each arm were extracted. These are compared with the EPC code calculations and the normalization factors were derived. Assuming the obtained normalization factor for the hadron production rate at the forward angles, singles rates of the counters in the proposed setup were evaluated.

The HES spectrometer will be vertically tilted by about 8 degrees which corresponds to 4 degrees of the electron scattering angle, so that the bremsstrahlung / M$\phi$ller electrons do not enter the spectrometer acceptance. The components of the focal plane detector system will be redesigned taking full advantage of existing resources.

A newly fabricated splitter magnet with a wider gap will be used, matching the HKS-HES geometrical acceptance.

The configuration and specification of the proposed hypernuclear spectrometer system is summarized in Table 1 and a schematic view is given

Table 1: Experimental condition and specification of the hypernuclear spectrometers

| | |
|---|---|
| **Beam condition** | |
| Beam energy | 2.5 GeV |
| Beam momentum stability | $3 \times 10^{-5}$ (rms) |
| **General configuration** | New Splitter +HKS spectrometer + HES spectrometer |
| **HKS spectrometer** | |
| Configuration | Q-Q-D and horizontal 70° bend |
| Central momentum | 1.2 GeV/$c$ |
| Dispersion | 4.7 cm/% |
| Momentum acceptance | $\pm$ 12.5% (1.05-1.35 GeV/$c$) |
| Momentum resolution ($\Delta p/p$) | $2 \times 10^{-4}$ |
| Solid angle | 10 msr with the new splitter<br>(30 msr without splitter) |
| Kaon detection angle | Horizontal : 7 degrees (1-13°) |
| Flight path length | 10 m |
| Maximum magnetic field | 1.6 T (normal conducting magnet) |
| **HES spectrometer** | |
| Configuration | Q-Q-D and horizontal 50° bend |
| Central momentum | 1.0 GeV/$c$ |
| Dispersion | 3.3 cm/% |
| Momentum acceptance | $\pm$ 15 % |
| Momentum resolution ($\delta p/p$) | $2 \times 10^{-4}$ |
| Solid angle | 10 msr with the new splitter |
| Electron detection angle | Horizontal : 0 degrees<br>Vertical : 4.5 degrees |
| Maximum magnetic field | 1.6 T (normal conducting magnet) |

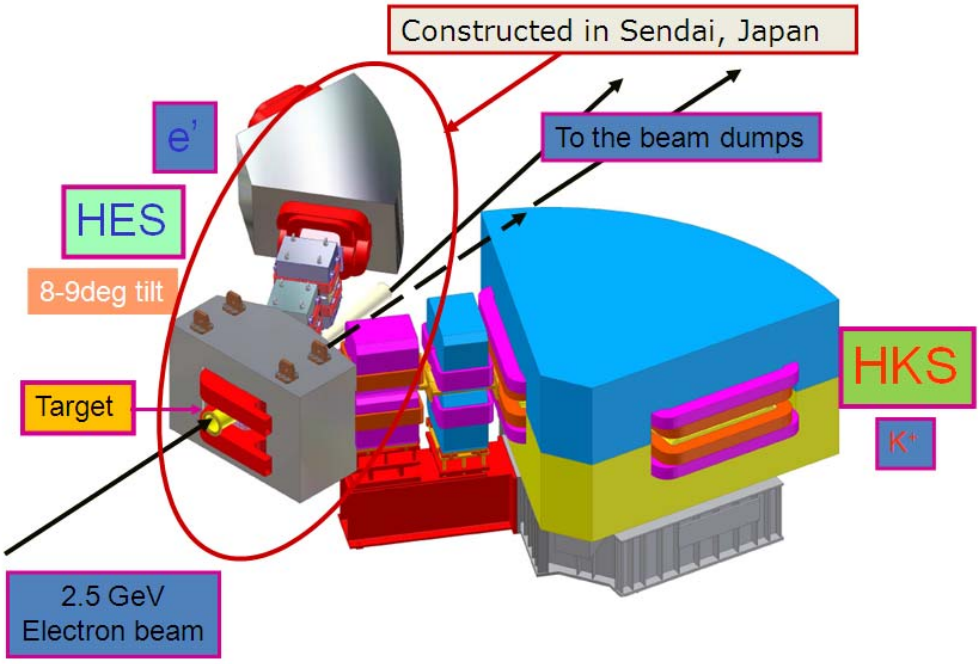


Figure 8: Schematic view of the setup for the proposing experiment.

in Figure 8.

### 3.2 Proposed reactions

The third generation experiment E05-115 requested 30 days of beamtime for:

1. HKS, HES spectrometers commission data, including the calibration data by p(e,e′K$^+$)$\Lambda, \Sigma^0$ and $^{12}$C(e,e′K$^+$)$^{12}_{\Lambda}$B reactions.
2. $A \sim 50$ hypernuclear spectroscopy by the $^{51}$V(e,e′K$^+$)$^{51}_{\Lambda}$Ti reaction.
3. Feasibility study of heavy hypernuclear spectroscopy by the $^{89}$Y(e,e′K$^+$)$^{89}_{\Lambda}$Sr reaction.
4. Spectroscopy of $p$-shell hypernuclei, selecting a few targets from $^{6,7}$Li and $^{10,11}$B.

The experiment was approved for 20 days of running, which in all likelihood will not allow for enough time on the light targets. Also, the experience gained from the E01-011 analysis leads us to request additional days for more sophisticated calibrations. Taking this and the earlier

discussed recent progresses in theory into account, we would like to propose the following reactions for the extension beam time.

1. **p(e,eK$^+$)$\Lambda, \Sigma^0$ and $^{12}$C(e,e′K$^+$)$^{12}_{\Lambda}$B reactions**

   The p(e,eK$^+$)$\Lambda, \Sigma^0$ and $^{12}$C(e,e′K$^+$)$^{12}_{\Lambda}$B reactions will be periodically measured over the entire beamtime in order to calibrate the absolute missing mass scale with a water cell ($H_2O$) or $CH_2$ targets. With the help of the JLab target group, the collaboration is now designing a water cell target, which is much simpler than the water fall target used for the Hall-A hypernuclear experiment. A water cell with thin metal windows will be placed in the target cooling water line. With the known $\Lambda$, $\Sigma^0$, $^{12}_{\Lambda}$B (g.s.) masses, the kaon and electron spectrometer system and primary electron beam energy are calibrated so that the absolute scale of the binding energy can be precisely determined. Since we aim to determine the absolute binding energies of a $\Lambda$ hyperon in a mass region where no emulsion experiments exist, those reactions are essential for the present experiment. It is in contrast to the $(\pi^+, \mathrm{K}^+)$ reaction in which we have to rely on other indirect reactions since a neutron target is not available. The $H_2O$ target will simultaneously provide $^{16}_{\Lambda}$N data as well as calibration data. We have a future plan to measure $\Lambda$-N scattering length through the final state interaction by using a cryogenic $D_2$ target. If beamtime allows, $H_2O$ can be replaced by $D_2O$ to study the feasibility of such an experiment.

   We request 3 additional days for continuous monitoring of the calibration while taking data for the primary targets listed below. Further, we request 2 additional days for more sophisticated calibration runs, like sieve slit data, beam energy scan, and spectrometer momentum scans (delta scans).

2. **$^{40}$Ca(e,e′K$^+$)$^{40}_{\Lambda}$K reaction**

   The $^{40}$Ca target is doubly $LS$-closed up to the $0d_{3/2}$ shell. As shown in Figure 3, $^{40}_{\Lambda}$K's natural parity states of $2^+, 3^-, 4^+$ are expected to be populated predominantly. Therefore, we can extract $s^{\Lambda}_{1/2}, p^{\Lambda}_{3/2}$ and $d^{\Lambda}_{5/2}$ energies with less ambiguity. For $A$-dependence study of $\Lambda$ single particle energies, it is important to have reliable $A = 40$ data to complete systematic study of hypernuclei in wide mass range, since we have or will have data for $A < 10$ $^{6,7}$Li, $^{10,11}$B; $10 < A < 20$ $^{12}$C, $^{16}$O; $A \sim 30$ $^{28}$Si; $A \sim 50$ $^{52}$Cr and only the $A \sim 40$ target is missing.

The $^{52}$Cr target has the closed neutron $f_{7/2}$ shell and quite stable because $N$=28. Physics motivation is quite similar to it for $^{51}$V target, but $^{52}_{\Lambda}$V has much simpler energy spectrum, since spectroscopic factor of the $^{51}$V is unmeasurably small by $^{52}$Cr(d,$^3$He)$^{51}$V. The extraction of effective $\Lambda$ binding potential depth would be easier for $^{52}$Cr target, though more complicated structure could be expected for $^{51}$V target. As the $A \sim 50$ target, we will spend the approve E05-115 beamtime for $^{52}$Cr rather than for $^{51}$V target which was proposed in the original E05-115 due to simpler structure of the expected $^{52}_{\Lambda}$V spectrum.

3. **$^{7}$Li(e,e′K$^+$)$^{7}_{\Lambda}$He and $^{10}$B(e,e′K$^+$)$^{10}_{\Lambda}$Be reactions**

   The $p$-shell $\Lambda$ hypernuclei have been intensively studied both experimentally and theoretically.

   Recently, there is an increasing interest in the $\Lambda N$-$\Sigma N$ coupling that is a source of $\Lambda NN$ three-body force and it is especially important in high-density neutron matter [5, 21]. It naturally plays a more significant role in the neutron-excess $\Lambda$ hypernuclei and it is indispensable to spectroscopically study the structure of $p$-shell $\Lambda$ hypernuclei for various isospins. For example, $^6$He is the lightest and also most simple two neutron halo nucleus. It is also one of the so called Borromean nuclei, *i.e.* either removal of one of the two halo neutrons or the alpha core leads to an unbound system. Like for other light Borromean and halo nuclei, its excited states are unbound. According to precise few body calculations [7], the unbound excited neutron halo states of $^6$He will be bound in $^{7}_{\Lambda}$He. Direct measurement of the $\Lambda$'s glue role is quite interesting.

   With its $\alpha + \alpha + n + \Lambda$ structure, $^{10}_{\Lambda}$Be is of similar interest, inasmuch as its $^9$Be core, too, is one of the Borromean nuclei, and it also does not exhibit a bound excited state. Furthermore, the $\Lambda$-$N$ potential established for $p$-shell hypernuclei could not explain the structure of $^{10}_{\Lambda}$B system, whose $^9$B core again is a Borromean nucleus, but not even bound in the ground state. The above $\Lambda$-$N$ interaction may have a room for improvement in tensor force part [7],and thus further investigation about the $\Lambda$-N tensor force is important. A systematic study of the $A = 10$ system is essential and the $^{10}$B(e,e′K$^+$)$^{10}_{\Lambda}$Be reaction will provide complementary information to $^{10}_{\Lambda}$B.

   The beamtime approved in the original E05-115 is not enough for the

precise measurement of the $\Lambda$'s glue role in the bound states of neutron halo nuclei, and thus, we would like to request additional beamtime, 3 days each on $^{7}$Li and $^{10}$B targets.

It should also be noted here that the (e, e′K$^{+}$) reaction has an advantage over meson induced reactions, because small and thin, enriched targets can be used due to the small beam size and high intensity of the primary electron beam. The enriched $^{10}$B targets of 100 mg/cm$^{2}$ thickness have been specially prepared with a double-stage sintering method.

# 4 Experimental setup and expected performance

In this section, we describe the proposed experimental setup and expected performance based on the latest simulation studies. It should be noted that all the listed equipments are already part of the approved E05-115 configuration.

## 4.1 General configuration

Our experimental setup consists of 1) the HKS spectrometer for the kaons, 2) the newly developed HES spectrometer for the electrons and 3) the new splitter for positive/negative charged particles separation.

In the following subsections, each spectrometer will be explained.

## 4.2 High resolution Kaon spectrometer (HKS)

General specifications of the HKS spectrometer are given in Table 1. In combination with new splitter, the HKS is designed to achieve simultaneously $2 \times 10^{-4}$ momentum resolution and about 10 msr solid angle acceptance over a momentum range of 1.2 GeV/$c \pm 12.5$%. The HKS is placed rotated horizontally such as to accept 1.2 GeV/$c$ K$^{+}$ with $\theta_K$ = 7° as a central ray in order to avoid zero degree positive particles, mostly positrons.

The detector system for HKS is summarized in Table 2. As seen in Table 4, the HKS singles rate is dominated by pions and protons, whose rate would be up to a few 100 kHz to a few MHz depending on the targets and beam currents. In order to achieve efficient pion rejection as high as $10^{-4}$, three layers of aerogel Čerenkov counter with refractive index of 1.055 were

installed. For proton rejection, two layers of water Čerenkov counter doped with a wavelength shifter were used so that the Čerenkov counter has good efficiency for the wide range of incident angles. During the E01-011 beamtime, we observed a gradual decrease in the number of photoelectrons of the water Čerenkov counters. We are now designing new water tanks for easy water exchange and better reflection efficiencies of photons. Time resolution of as good as 80 ps is a goal for the time-of-flight scintillators. The good time resolution will enable us to identify kaons at the off-line analysis without detailed momentum reconstruction. The tracking chambers of HKS have high rate capability and accept the rates of up to a few MHz. Those detectors were commissioned in the E01-011 experiment. Another layer of lucite Čerenkov counters will be added just behind the water Čerenkov to have better proton rejection and longer flight path for time-of-flight measurement. Design and fabrication of the lucite Čerenkov counters are now in progress.

### 4.3 High-resolution electron spectrometer (HES), the new e′ spectrometer

The collaboration finished fabrication of the HES magnets and the new splitter. Field mapping of the magnets has been completed in Japan and they will arrive at JLab in February 2008.

The HES consists of Q-Q-D magnets and it is basically a smaller version of the HKS (Table 1). The central momentum for the HKS is fixed at 1.2 GeV/$c$, and thus, the central momentum of the HES should be adjusted once the primary electron beam energy is decided. Therefore, the scattered electron emission angle and the installation position of HES depends on the primary beam energy. Though the HKS + HES + new SPL system can accept 2.1$\sim$2.5 GeV beam energy, but a beam energy of 2.46 GeV is optimum and our simulation based on it.

The “tilt method” will be applied to the HES as first introduced to the Enge spectrometer in E01-011. The tilt angle depends on the e′ momentum, and thus, we fabricated a tilt angle adjustable support system with hydraulic jacks for the HES.

With increasing e′ momentum, the scattering angles of the corresponding M$\phi$ller electrons become smaller. Therefore, we have a chance to make the tilt angle smaller, where the virtual photon flux is larger, to the limit of the e′ detector operation. With data obtained in E01-011, we optimized tilt angle

Table 2: Detectors for the HKS spectrometer

| Nomenclature | Size | Comments |
|---|---|---|
| *Drift chamber* | | |
| HDC1 | $30^H \times 120^W \times 14^T cm^3$ | xx'uu'(+30 deg)vv'(-30 deg) |
| | | 5 mm drift distance |
| HDC2 | $30^H \times 120^W \times 14^T cm^3$ | xx'uu'(+30 deg)vv'(-30 deg) |
| | | 5 mm drift distance |
| *Time of flight wall* | | |
| HTF1X | $30^H \times 125^W \times 2^T cm^3$ | $7.5^W$ cm $\times$ 17-segments, H1949 |
| HTF1Y | $30^H \times 125^W \times 2^T cm^3$ | $3.5^W$ cm $\times$ 9-segments, H1949 |
| HTF2X | $35^H \times 170^W \times 2^T cm^3$ | $9.5^W$ cm $\times$ 18-segments, H1949 |
| *Čerenkov counter* | | |
| HAC1 | $46^H \times 169^W \times 31^T cm^3$ | n = 1.055 hydrophobic aerogel |
| | | 14 $\times$ 5" PMT (7 seg.) |
| HAC2 | $46^H \times 169^W \times 31^T cm^3$ | n = 1.055 hydrophobic aerogel* |
| | | 14 $\times$ 5" PMT |
| HAC3 | $46^H \times 169^W \times 31^T cm^3$ | n = 1.055 hydrophobic aerogel |
| | | 14 $\times$ 5" PMT |
| HWC1 | $35^H \times 187.2^W \times 8^T cm^3$ | $15.6^W$ cm $\times$ 12-segments, H1161 * |
| | | Water with wavelength shifter |
| HWC2 | $35^H \times 187.2^W \times 8^T cm^3$ | $15.6^W$ cm $\times$ 12-segments, H1161 |
| | | Water with wavelength shifter |
| LC | $45^H \times 189^W \times 2.5^T cm^3$ | $13.5^W$ cm $\times$ 14-segments, photonics 3" tube |

* HACs will be staggered to each other. HWCs will be so.

and offset of the HES system as a function of incoming beam energy.

We will re-use the honeycomb cell structured drift chamber (EDC1), which was used for Enge in E01-011. Another planer drift chamber, which was fabricated as a spare chamber for the HKS DC, will be placed as EDC2. The plastic scintillator hodoscopes will be newly designed to cover a larger area. Detector parameters are summarized in Table 3. The readout electronics and analysis techniques have already been established in the E01-011 experiment.

### 4.4 Singles rates

Count rates in the HKS and HES spectrometers were estimated as follows:

1. The rates of $e^+$, $\pi^+$ and proton for $^7$Li, $^{10}$B, $^{12}$C, $^{89}$Y were measured in E01-011. The beam energy difference (E01-011: 1.851 GeV, E05-115:

Table 3: Detectors for the HES spectrometer

| Nomenclature | Size | Comments |
|---|---|---|
| | *Drift chamber* | |
| EDC1 | $12^H \times 100^W \times 30^T cm$ | Honeycomb cell, xx'uu'vv'xx'uu'vv'xx' ($\pm 30^\circ$) |
| EDC2 | $30^H \times 120^W \times 14^T cm$ | xx'uu'vv' ($\pm 30^\circ$) |
| | *Hodoscope* | |
| EHOD1 | $30^H \times 117^W \times 1^T cm$ | 29 segmentation |
| EHOD2 | $30^H \times 117^W \times 1^T cm$ | 29 segmentation staggered to EHOD1 |

2.460 GeV) was corrected with the cross sections calculated by the EPC code. A correction factor for the solid angle of the HKS was obtained by a GEANT4 simulation.

2. Quasi-free kaon production rates were measured for $^{7}$Li, $^{10}$B, $^{12}$C, $^{51}$V in E01-011 and their values are normalized to the new SPL + HKS solid angle. Quasi-free kaon production cross sections for $^{40}$Ca, $^{52}$Cr were assumed to scale as $A^{0.8}$ which is roughly consistent with the E01-011 data.

3. Measured electron rates in Enge were normalized to HES by using GEANT4 simulations. Event generation was carried out by two methods, one by the EGS code and the other by the Lightbody code, which agreed more or less to each other. The rate of $\pi^-$ was calculated by the EPC code with the same normalization factor as for the hadron arm.

As seen in Table 4, the singles rate of HKS is dominated by $\pi^+$s and protons, while that for HES is by electrons. It should be noted that we expect the positron rate in HKS to be low since we setup HKS at an angle off 0 degrees. The singles rate of the HES hodoscope is expected almost two orders of magnitude less than that of E89-009. With this rate, the hardware coincidence between electron arm and kaon arm can form good triggers.

### 4.5 Resolution of excitation energy spectra

The following factors contribute to the total resolution of the experiment:

1. HKS momentum, angular resolution

Table 4: Singles rates

| Target | Beam Intensity ($\mu$A) | HKS $e^+$ rate (kHz) | HKS $\pi^+$ rate (kHz) | HKS $K^+$ rate (Hz) | HKS $p$ rate (kHz) | HES $e^-$ rate (MHz) | HES $\pi^-$ rate (kHz) |
|---|---|---|---|---|---|---|---|
| $^{7}$Li | 15 | 0.2 | 5.4 | 68 | 7.6 | 0.5 | 1.1 |
| $^{10}$B | 30 | 0.7 | 44 | 164 | 33 | 0.9 | 2.0 |
| $^{12}$C | 50 | 1.4 | 13 | 161 | 21 | 1.8 | 2.8 |
| $^{40}$Ca | 10 | 0.9 | 3.2 | 27 | 4.9 | 1.0 | 0.7 |
| $^{52}$Cr | 30 | 3.1 | 9.7 | 79 | 13 | 3.4 | 2.1 |

We performed GEANT Monte Carlo simulations with a 3-dimensional magnetic field map calculated by TOSCA; this provides the angular resolution of the HKS. A momentum resolution of $2 \times 10^{-4}$ for the HKS was assumed and these contributions were projected on the missing mass. Kinematic broadening effects due to the uncertainty of the $K^+$ scattering angle was included in the simulation.

2. HES momentum, angular resolution
   A GEANT simulation with 3D magnetic field of the HES was performed. The momentum resolution of $2 \times 10^{-4}$ for the HES was assumed.

3. Beam energy spread
   A beam energy spread of $\sigma = 3 \times 10^{-5}$ corresponds to 175 keV (FWHM) for 2.5 GeV beam and its contribution to the missing mass was calculated.

4. Energy loss in the target
   The energy losses in the target (100 mg/cm$^2$) were estimated with GEANT simulations for $K^+$, e$'$ and the primary beam. The obtained energy losses were converted to the contribution to the mass resolution. We assumed that the correction can be done with an accuracy of $<$50% of the energy loss itself.

The results are summarized in Table 5. The present proposed experiment is expected to achieve a resolution of $\sim$350 keV (FWHM).

### 4.6 Background and signal/noise ratios

One of the major sources of background in the proposed setting that facilitates detection of very forward particles is electrons associated with

Table 5: The energy resolution of the HKS system

| Item | Contribution to resolution (keV, FWHM) | | | | |
|---|---|---|---|---|---|
| Target | Li | B | C | Ca | Cr |
| HKS momentum | 211 | 214 | 216 | 220 | 220 |
| HKS angle | 36 | 26 | 21 | 7 | 5 |
| HES momentum | 184 | 187 | 188 | 192 | 192 |
| HES angle | 45 | 32 | 27 | 8 | 6 |
| Beam momentum | 166 | 168 | 169 | 172 | 173 |
| Energy loss | $<$97 | $<$106 | $<$105 | $<$96 | $<$85 |
| Overall | **345** | **350** | **350** | **353** | **350** |

bremsstrahlung and M$\phi$ller processes. We suppress these background by the "tilt method", which offers us 50 times more hypernuclear yield and a factor of 10 better signal to noise ratio compared to the E89-009 setup.

Table 6: Expected hypernuclear production rates in the (e,e$'$K$^+$) reaction

| Target | beam Intensity ($\mu$A) | Hyp.Nucl. per 100nb/sr $\cdot$ hour | Qfree K$^+$ in HKS(Hz) | B.G. level in 200 keV nb/sr equiv. |
|---|---|---|---|---|
| $^{7}$**Li** | 15 | 48 | 68 | 2.6 |
| $^{10}$**B** | 30 | 67 | 164 | 8.6 |
| $^{12}$**C** | 50 | 93 | 161 | 12 |
| $^{40}$**Ca** | 10 | 6 | 27 | 18 |
| $^{52}$**Cr** | 30 | 13 | 79 | 81 |

Electron and positron rates were estimated as given in Table 4. For example, 1.8 MHz of the electron background is expected in the HES spectrometer assuming 2.46 GeV, 50 $\mu$A electron beam and 100 mg/cm$^2$ $^{12}$C target. Kaon singles rate for the HKS spectrometer was estimated to be 161 Hz for the $^{12}$C target. With a coincidence window of 2 ns, we have an accidental coincidence rate of:

$$N_{ACC} = (1.8 \times 10^6 \mathrm{Hz}) \cdot (2 \times 10^{-9} \mathrm{sec}) \cdot (161 \mathrm{Hz}) \sim 0.58/\mathrm{sec}.$$

Assuming that the accidental coincidence events spread uniformly over the momenta space (HES 300 MeV/$c$ $\times$ HKS 240 MeV/$c$), the largest background per bin (200 keV) projected on the hypernuclear mass is 6.3 $\times$ $10^{-4}$ /sec. A typical hypernuclear ($^{12}_{\Lambda}$B$_{g.s.}$, 140 nb/sr, 50$\mu$A beam) event rate

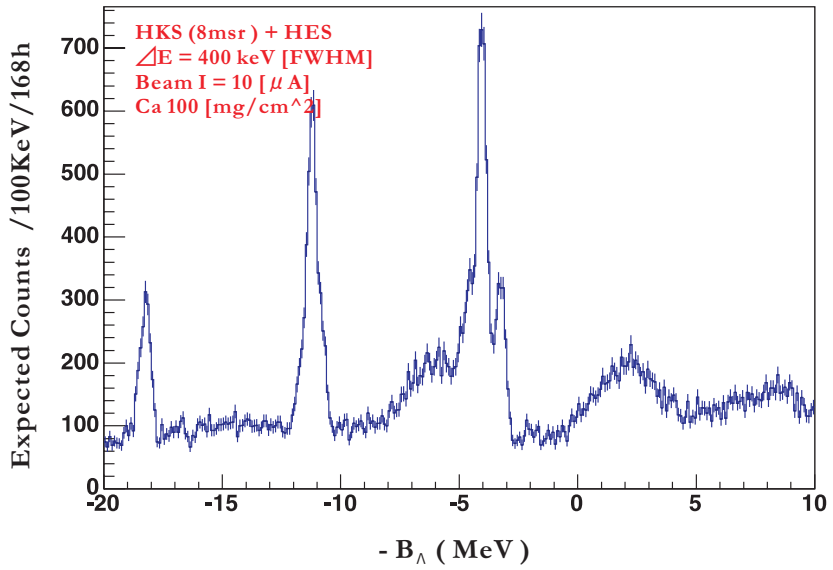


Figure 9: An expected $^{40}$Ca(e,e′K$^+$)$^{40}_{\Lambda}$K spectrum. The HKS-HES acceptance was taken into accout in the GEANT simulation. Quasi-free events expected in $-B_\Lambda > 0$ are not included.

will be,

$$93/(100\mathrm{nb/sr})/\mathrm{h} \times 140\ \mathrm{nb/sr} = 3.6 \times 10^{-2}/\mathrm{sec}.$$

Assuming Gaussian peak shape and an energy resolution of 400 keV, about 20% of the total events will be in a 200 keV bin, and thus S/N is estimated as $\sim$11. Table 6 summarizes hypernuclear production rates for 100 nb/sr and quasi-free K$^+$ rates. The background levels in a 200 keV bin are also shown in terms of the cross section that a Gaussian peak (400 keV FWHM) with $S/N = 1$ would correspond to.

Figure 9 is an expected $^{40}_{\Lambda}$K spectrum with 100 mg/cm$^2$ $^{40}$Ca target, 10$\mu$A beam intensity, and 168 hours of beamtime.

# 5 Calibration procedures

Although ultimately successful, the E01-011 off-line calibration procedure was very complicated and time consuming. High quality calibration data are essentially important to control systematic errors as well as to make analysis simpler and more reliable. One of great advantage of the (e,e′K$^+$) reaction with spectrometers with large momentum acceptance, like HKS and HES, is that the absolute energy scale can be calibrated by the p(e,e′K$^+$)$\Lambda$, $\Sigma^0$ reactions. During E01-011, we performed the following calibration measurements:

1. Using protons in the $CH_2$ target, we took data for p(e,e′$K^+$)$\Lambda$, $\Sigma^0$ reactions and calibrated the missing mass scale with the known $\Lambda, \Sigma^0$ masses.

2. Sieve slit runs with a single arm trigger for each of HKS and Enge spectrometers were taken to extract the angular reconstruction matrices.

3. Using the $^{12}$C target, data of the ground state of the $^{12}_{\Lambda}$B hypernucleus were taken for the calibration as well as for physics motivation.

Let us explain what additional calibration methods we would like to use in here the proposed extension to the E05-115 experiment.

**Water cell target**

One problem of the $CH_2$ target is that it cannot sustain high current ($> 2\ \mu$A) electron beam. Hydrogen escapes from the target and the target was finally burnt out even with large beam raster ($5 \times 5$mm$^2$) . This made a reliable extraction of the $\Lambda, \Sigma^0$ electro-production cross sections almost impossible. Though these cross sections are not necessary for the energy calibration, they are fundamental and quite interesting physics quantities by themselves.

We monitored the $\Lambda$ production rate in E01-011 and we replaced the target by a new one when the rate became 60% of the original value. Short lifetime and difficulty in frequent changes of the $CH_2$ target prevented us from periodical missing mass calibrations, which is important to control systematic errors from the beam energy drifts, magnetic field fluctuation and other time dependent effects. To avoid this problem, we will introduce a water cell target.

In E01-011, we used target ladders with six pockets which accept solid targets. As shown in Figure 10, we are considering to make a ladder with water cooling pipes and a water cell. By using the water cell target, we can take $H_2O$ data once in every shift and thus time dependent systematic errors will be well controlled. Furthermore, ambiguities from the large beam raster can be avoided.

Beam raster effects have not been studied well in E01-011. Therefore, there was little room for an optimization of the correction function. Hopefully, we can avoid large raster for the $CH_2$ target by introduction of the water target, however, fragile, low-melting-point solid targets ($^{10,11}$B,

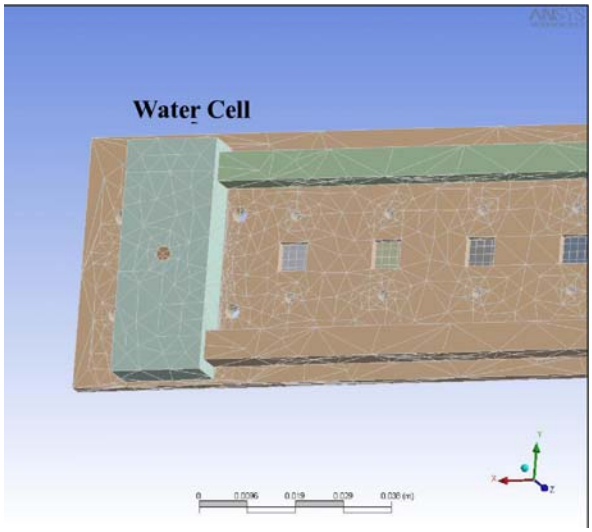


Figure 10: Schematic figure of a target ladder with a water cell. Pockets can accept $1 \times 1\text{cm}^2$ solid targets and one of them is replaced by a water cell which is connected to cooling water pipes.

$^{6,7}$Li) may still need a small raster. We can take the water data with and without the raster to have information about the raster correction matrices.

The water cell target enables us to use a proton in $H_2O$ without problems from hydrogen escape and simultaneously to study $\Lambda, \Sigma^0$ electro-production cross sections and $^{16}_{\Lambda}$N spectroscopy. Heat calculation by the finite element method and a prototype target cell fabrication are now in progress.

### Sieve slit runs

In E01-011, we took sieve slit data with the $^{12}$C target for each arm in order to calibrate angles. Our sieve slits are placed between the splitter magnet and the two spectrometers, and thus, momenta and angles are correlated even for particles that pass through the same hole. Thus, the analysis is not as straightforward as with sieve slits placed just after the target in front of any dispersive element. However, our sieve slits still provide quite a strong constraint on the transfer matrices. Therefore, we will take again single arm sieve slit data during the commissioning period of the proposed experiment.

By introducing the water cell target, $\Lambda$ tagging sieve slit runs become possible. During p(e,e$'$K$^+$)$\Lambda$ data taking, the sieve slit can be inserted in one arm. This was impossible with the $CH_2$ target due to beam current limitations.

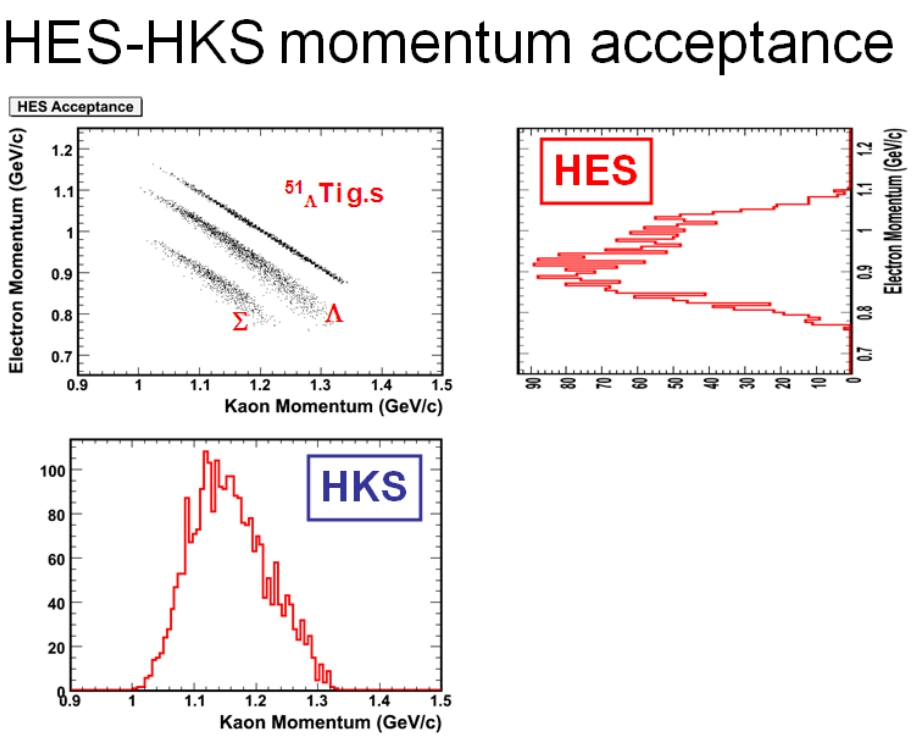


Figure 11: Momentum acceptance of HKS and HES with missing mass distributions for $\Lambda$, $\Sigma^0$ and ${}^{51}_{\Lambda}$Ti hypernucleus.

Figure 11 shows the correlated $P_{K^+}$ vs. $P_{e'}$ momentum acceptances of HKS and HES for $\Lambda$, $\Sigma^0$, and ${}^{51}_{\Lambda}$Ti hypernucleus. Using periodical data taking with the water cell target and the ${}^{12}$C target, the missing mass scale will be always calibrated along these correlated lines in the $P_{K^+} - P_{e'}$ space. However, they do not cover the entire acceptance of the HKS-HES system.

This correlation can be moved by changing 1) the primary electron beam energy ($E_e$), 2) the momentum acceptance of HKS, and 3) the momentum acceptance of HES.

Therefore, just after commissioning of the HKS and HES spectrometers, we would like to 1) scan $E_e$, 2) scale magnetic fields of the HKS magnets, and 3) scale magnetic fields of the HES magnets, in order to move the correlations in the $P_{K^+} - P_{e'}$ space.

These calibrations will ensure the differential linearity of $P_{K^+}$ and $P_{e'}$ during the spectrometers' matrices tune. Once the correlation covers the entire momentum space, the absolute missing mass calibration will be provided by periodical $\Lambda, \Sigma^0$ and ${}^{12}_{\Lambda}\mathrm{B}_{gs}$ peaks, and thus it is enough to scan just once before the physics runs.

With the help of the JLab accelerator group, the collaboration will seek also a possibility to take data of the elastic scattering for the single arm momentum calibration.

# 6 Yield estimate and requested beam time

The expected yield of the hypernuclear states are evaluated based on the E89-009 and E01-011 results for the ${}^{12}_{\Lambda}$B ground state in the ${}^{12}$C(e,e′K$^+$)${}^{12}_{\Lambda}$B reaction. In E01-011, the "tilt method" reduced the background effectively, and for E05-115 we are expecting more than 50 times the hypernuclear yield rate gain obtained from E89-009 and a 5 times gain over E01-011. This is partly because we can use higher intensity beams and thick targets and partly because the kaon spectrometer has a larger solid angle acceptance and better momentum matching with the electron spectrometer.

The cross sections of the hypernuclear states have been calculated for ${}^{7}$Li [18], ${}^{10}$B [19, 20] and ${}^{40}$Ca, ${}^{52}$Cr [17]. They are listed in Table 7.

It should be noted, however, that the calculated cross sections could vary by a factor of 2-5 depending on the choice of model parameters for the elementary reaction, the hypernuclear potentials, the configuration of the states. In the present yield estimate for the beamtime request, the cross sections were normalized assuming the cross section of the ${}^{12}$C(e,e′K$^+$)${}^{12}_{\Lambda}$B reaction for the ground state doublet is 100 nb/sr.

The 5 days of calibration beamtime includes the initial beam studies such as $E_e, P_{e'}, P_{K^+}$ scans, sieve slit runs as well as periodical $H_2O$, ${}^{12}$C calibration runs during entire beamtime. It should be noted that beamtime for the periodical calibration is in proportion to the beamtime for additional physics runs and we cannot squeeze this calibration time in the approved E05-115 beamtime, if additional physics beamtime is approved.

The requested data taking hours were calculated so that more than 800 counts for the $s^{\Lambda}_{1/2}$ state of ${}^{40}_{\Lambda}$K are accumulated to determine the peak center with an accuracy of 15 keV. For excited levels of $p$-shell hypernuclei, ${}^{7}_{\Lambda}$He and ${}^{10}_{\Lambda}$Be, the beamtime were estimated to have more than 200 counts for excited states assuming the cross sections in Table 7. A 60% efficiency was assumed for data taking and data analysis.

The data taking for ${}^{52}$Cr, ${}^{6}$Li, ${}^{11}$B targets will be carried out within the originally approved E05-115 beamtime.

The collaboration prepared the enriched targets of ${}^{10,11}$B with a thickness

Table 7: Cross sections of ${}^{7}_{\Lambda}$He, ${}^{10}_{\Lambda}$Be, ${}^{40}_{\Lambda}$K and ${}^{52}_{\Lambda}$V calculated by DWIA [17, 18, 19]

| Target | Hypernucleus | Hypernuclear configuration | Cross section (nb/sr) |
|---|---|---|---|
| ${}^{7}$Li | ${}^{7}_{\Lambda}$He | $s^{\Lambda}_{1/2}, 1/2^{+}$ | 21 |
| | | $s^{\Lambda}_{1/2}, 5/2^{+}, 3/2^{+}$ | 9 |
| ${}^{10}$B | ${}^{10}_{\Lambda}$Be | $s^{\Lambda}_{1/2}, 2^{-}, 1^{-}$ | 21 |
| | | $s^{\Lambda}_{1/2}, 3^{-}, 2^{-}$ | 15 |
| | | $s^{\Lambda}_{1/2}, 4^{-}, 3^{-}$ | 18 |
| ${}^{40}$Ca | ${}^{40}_{\Lambda}$K | $s^{\Lambda}_{1/2}, 2^{+}$ | 84 |
| | | $p^{\Lambda}_{3/2}, 3^{-}$ | 208 |
| | | $d^{\Lambda}_{5/2}, 4^{+}$ | 248 |
| ${}^{52}$Cr | ${}^{52}_{\Lambda}$V | $s^{\Lambda}_{1/2}, 4^{-}, 3^{-}$ | 69 |
| | | $p^{\Lambda}_{3/2}, 5^{+}, 4^{+}$ | 160 |
| | | $d^{\Lambda}_{5/2}, 6^{-}, 5^{-}$ | 198 |
| | | $f^{\Lambda}_{7/2}, 7^{+}, 6^{+}$ | 148 |

of about 100 mg/cm$^2$ and enriched $^{40}$Ca and $^{6,7}$Li will be prepared with help of the JLab target group. The requested beamtime is summarized in Table 8. Requested beam conditions are listed in Table 9.

# 7 Schedule of the spectrometer construction and requested support

The HKS spectrometer is now stationed at the parking position in Hall C, and it can be moved to the operating position without major work.

The disassembled HES magnets will be delivered to JLab in February, 2008. They will be assembled on the movable platform in Hall C during a beam break and stored in Hall C until the beamtime. Power supplies for the HKS-dipole and HES-dipole are provided by the collaboration. DC power supplies for the other HKS and HES magnets and the SPL are requested to be provided by JLab. Since the detectors for the HES are almost the same as those for the Enge spectrometer, we see no difficulty to construct them and test them using cosmic rays and available accelerator beams ($eg.$ LNS-Tohoku) before we receive the beam at JLab.

All the above requests are for the approved E05-115 experiment and the proposed additional beamtime will not demand any extra major work.

Table 8: Requested beamtime in addition to approved E05-115 beamtime (20 days).

| | Target | Hypernucleus | Number of days | Number of hours |
|---|---|---|---|---|
| $E_e, P_{e'}, P_K$ scans and S.S. runs | | | 2 | 48 |
| Periodical Calibration | $H_2O$, $^{12}C$ | $\Lambda, \Sigma^0$ $^{12}_{\Lambda}B$, $^{16}_{\Lambda}N$ | 3 | 72 |
| **Total for calibration** | | | 5 | **120** |
| Physics runs | $^{7}Li$ | $^{7}_{\Lambda}He$, | 3 | 72 |
| | $^{10}B$ | $^{10}_{\Lambda}Be$ | 3 | 72 |
| | $^{40}Ca$ | $^{40}_{\Lambda}K$ | 7 | 168 |
| **Total for data taking** | | | 13 | **312** |
| **Grand Total** | | | 18 | **432** |

Table 9: Requested beam conditions

| | |
|---|---|
| Typical beam energy | 2.46 GeV |
| Typical beam current | 10$\sim 50$ $\mu$A |
| Beam energy stability | $\leq 3 \times 10^{-5}$ |

# 8 Summary

Based on recent progresses in theoretical studies and analysis/calibration procedures, high-resolution (e,e′$K^+$) spectroscopy for $^{40}$Ca, $^{7}$Li and $^{10}$B and new calibration methods have been proposed and additional beamtime has been requested in addition to the approved E05-115 beamtime. By the proposed experiment, we plan to reveal 1) $\Lambda N$-$\Sigma N$ coupling effects in the $\Lambda$-$N$ interaction, and 2) Single-particle nature of a $\Lambda$ hyperon by deriving single particle binding energies and widths and/or splitting of the single-particle states in the medium-heavy hypernuclei with simple-core structure.

The present proposal postulates that we use the high resolution kaon spectrometer (HKS) and the high-resolution electron spectrometer (HES) which were constructed by the Tohoku group using the budget of MEXT, Japan. The HES construction was finished and it will arrive at JLab at the beginning of 2008. The R&D work for detectors and simulation, analysis codes development are in progress for the approved E05-115 experiment. The proposed additional experiment needs no extra man-power and resources. The proposal is fully based on the success of the first generation E89-009, and the second generation E01-011 experiments carried out in

Table 10: Present expected time line for the installation.

| | |
|---|---|
| **April, 2007 - March, 2008** | |
| | Analysis of E01-011 data |
| | Construction of the HES magnets |
| | Field map of the HES magnets |
| | Design and construction of HES-Hodoscope |
| | Design and construction of new HKS water Čerenkov box |
| | Design of new HKS lucite Čerenkov counter |
| | Shipping of the HES magnets to JLab (**we are here**) |
| | Construction of the lucite Čerenkov counters |
| **April, 2008 - December, 2008** | |
| | Completion of the detector construction |
| | Commission of detectors at a test bench |
| | Polishing up of simulation and analysis codes |
| | Final result of E01-011 |
| **January, 2009** | |
| | Collaboration will be ready for installation of the spectrometers, commission and beamtime for data taking. |

2000 and 2005.

Once the proposed experiment is successfully performed, we envision that the next stage of the hypernuclear physics program by the (e,e′$K^+$) reaction will be fully explored as 1) Λ hypernuclear spectroscopy for targets as heavy as Pb; 2) Intensive high quality spectroscopy of light Λ hypernuclei with cryogenic targets; and also 3) Open the doorway to coincidence experiments taking advantage of high-quality high-power electron beam at Jefferson Laboratory.

# References


[1] B. Povh, *Prog. Part. Nucl. Physics* **18** (1987) 183.

[2] R. Chrien and C. Dover, *Ann. Rev. Nucl. Part. Sci.* **39** (1989) 113.

[3] H. Bandō, T. Motoba, J. Žofka, *Int. J. Mod. Phys.* **21** (1990) 4021.

[4] JLab Hall A and Hall C Hypernuclear Collaboration, *White paper on hypernuclear spectroscopy at Jefferson Lab*, January (2007).

[5] Y. Akaishi, T. Harada, S. Shinmura and Khin Swe Myint, *Phys. Rev. Lett.* **84** (2000) 3539.

[6] E. Hiyama, M. Kamimura, T. Motoba, T. Yamada and Y. Yamamoto *Phys. Rev. C* **53** (1996) 2075.

[7] E. Hiyama, *private communication, to be published* (2006).

[8] T. Yamada and K. Ikeda, *Phys. Rev. C* **46** (1992) 1315.

[9] A series of $\gamma$-ray spectrocopic experiments are summarized in O. Hashimoto and H. Tamura, *Prog. in Part. Nucl. Phys.* **57** (2006) 564.

[10] J. Millener, A. Gal, C.B. Dover, R.H. Dalitz, *Phys. Rev. C* **31** (1989) 449.

[11] T. Yamazaki
*Proc. KEK Int. Workshop on Nuclear Physics in the GeV region*, KEK Report 84-20 (1984) 3.

[12] K. Tsushima, K. Saito, J. Haidenbauer, A.W. Thomas, *Nucl. Phys. A* **630** (1998) 691.

[13] C.M. Keil, F. Hofmann, H.Lenske, *Phys. Rev. C* **61** (2000) 064309; H. Lenske, *presentation at HYP2006* (2006) Mainz.

[14] T. Motoba, H. Bandō, R. Wünsch and J. Zofka, *Phys. Rev. C* **38** 1322 (1988).

[15] C.B. Dover, *Proc. Int. Symp. on Medium Energy Physics*, Beijing, World Scientific, Singapore, (1987) 257.

[16] T. Motoba, *Private communication*.

[17] P. Bydzovsky, M. Sotona, T. Motoba, K. Itonaga, K. Ogawa and O. Hashimoto, *submitted to Phys. Rev. C*; arXiv nucl-th 0706.3836.

[18] M. Sotona and S. Frullani, *Prog. Thor. Phys. Suppl.* **117** (1994) 151.

[19] T. Motoba, M. Sotona and K. Itonaga, *Prog. Thor. Phys. Suppl.* **117** (1994) 123.

[20] M. Sotona $et\ al.$, *Proceedings of Mesons and Light Nuclei '98*, (1998) 207.

[21] S. Shinmura, Khin Swe Myint, T. Harada and Y. Akaishi, *J. Phys. G* **28** (2002) L1.